

Morphology, Molecular Phylogeny, and Ecology of *Binucleata daphniae* n. g., n. sp. (Fungi: Microsporidia), a Parasite of *Daphnia magna* Straus, 1820 (Crustacea: Branchiopoda)

DOMINIK REFARDT,^a ELLEN DECAESTECKER,^{b,c} PIETER T. J. JOHNSON^d and JIŘÍ VÁVRA^{e,f,1}

^aUnité Ecologie et Evolution, Université de Fribourg, Chemin du Musée 10, CH-1700 Fribourg, Switzerland, and

^bLaboratory of Aquatic Ecology and Evolutionary Biology, KULeuven, Ch. Debériotstraat 32, B-3000 Leuven, Belgium, and

^cLaboratory of Aquatic Biology, Interdisciplinary Research Center, KULeuven Campus Kortrijk, E. Sabbelaan 53, B-8500 Kortrijk, Belgium, and

^dDepartment of Ecology and Evolutionary Biology, N344 Ramaley, University of Colorado, 334 UCB, Boulder, Colorado, USA, and

^eBiological Centre of the Czech Academy of Sciences, Institute of Parasitology, České Budějovice, Czech Republic, and

^fFaculty of Biology, University of South Bohemia, České Budějovice, Czech Republic

ABSTRACT. We describe a new microsporidian species *Binucleata daphniae*, n. g., n. sp., that infects the integument cells lining the hemocoel cavity of the carapace and the postabdomen of the cladoceran *Daphnia magna* Straus. Infected cells filled with spores accumulate as large clusters in the carapace cavity and heavily infected hosts are detected by their opaque appearance. Despite the parasite's presence, infected *Daphnia* grow and molt, but have a reduced fecundity. During the parasite's life cycle, chain-like meronts with isolated nuclei are formed, giving rise to binucleate presporonts, the most frequently observed, characteristic developmental stage. In sporogony, the nuclei of the presporont separate, divide, and eight spores enclosed in a thin-walled sporophorous vesicle are formed. Spores are $4.9 \times 2.5 \mu\text{m}$ in size (fresh) and have an anisofilar polar filament with eight coils. DNA sequence analysis places *B. daphniae* in a clade of microsporidians that parasitize crustaceans and mosquitoes and have assumed complex life cycles. *Binucleata daphniae*, however, has a simple and direct life cycle and can be transferred to naïve hosts and maintained as persistent infections in populations of its host *D. magna*. We propose that *B. daphniae* has simplified its life cycle by losing its secondary host, rendering it unique in this clade.

Key Words. *Berwaldia*, Cladocera, *Gurleya*, *Larssonia*, *Senoma*, transmission, ultrastructure, virulence.

MICROSPORIDIA are a diverse group of parasitic protists with close ties to the fungi or fungi-like organisms (Fast, Logsdon, and Doolittle 1999; Hirt et al. 1999; James et al. 2006; Keeling 2003; Liu, Hodson, and Hall 2006). They commonly parasitize animal hosts, particularly crustaceans and insects. More than 1,200 species representing more than 130 genera have been described (Canning and Vávra 2002). Microsporidia are strictly intracellular parasites, the only life-cycle stage occurring outside the host is a structurally complex, unicellular spore, equipped with a unique apparatus to inject the parasite's cytoplasm and its nucleus into the host cell through an evaginable tube (Vávra and Larsson 1999).

Most microsporidians from terrestrial hosts have a simple life cycle with direct transmission. Transmission occurs between hosts via spores capable of infecting the same host species from which they were isolated (i.e. homoinfectious spores of Vávra et al. 2005). However, many microsporidians from aquatic arthropods, such as crustacea and insects with aquatic larvae, have spores that are not infective to the original host (i.e. heteroinfectious spores of Vávra et al. 2005) and microsporidians having such spores must be transmitted through another host to complete their life cycle. Such complex life cycles have been elucidated in a few species belonging to the genus *Amblyospora*, where the parasite alternates between a copepod and a mosquito phase (Becnel, White, and Shapiro 2005). Complete life cycles have not been elucidated for a number of aquatic microsporidians that produce heteroinfectious spores or belong to microsporidian clades whose members possess heteroinfectious spores.

The crustacean order Cladocera hosts a number of microsporidian species of several genera (Ebert 2005; Green 1974). These parasites are of polyphyletic origin, and include members from both the clade of aquatic microsporidians parasitizing crustaceans and mosquitoes, as well as terrestrial microsporidians parasitizing insects and vertebrates (Refardt et al. 2002; Vossbrinck et al. 2004; Vossbrinck and Debrunner-Vossbrinck 2005). Some of these parasites were shown to have heteroinfectious spores (Vávra 1964). Based on their phylogenetic position, it has further been suggested that some parasites of Cladocera have complex life cycles, possibly with a mosquito as the alternate host (Refardt et al. 2002). Cladoceran microsporidians have also proven an ideal model system to study the ecology of host-parasite interactions, the evolution of virulence, and epidemiology (Ebert 2005).

The present paper describes the morphology, molecular phylogeny and ecology of the microsporidian *B. daphniae* n. g., n. sp., *Binucleata* a parasite of the cladoceran *Daphnia magna* Straus, 1820. Such a comprehensive description is warranted because several features of *B. daphniae* are of general interest. First, *B. daphniae* is shown to have homoinfectious spores and direct transmission, yet it belongs to a clade whose members produce heteroinfectious spores. *Binucleata daphniae* may therefore be an example of a microsporidian parasite that has only recently in its evolutionary history abbreviated its life cycle from the complex to the simple. Second, the ease with which *B. daphniae* can be kept in co-culture with its host, its high infectivity and moderate virulence make it an attractive model system to study host-parasite interactions. Third, the parasite shows a remarkably fine-tuned interaction with its host during development. It infects the cuticular hypodermis, a tissue whose structural and physiological integrity is essential for host survival, while the host continues to grow and molt.

MATERIALS AND METHODS

Parasite origin and propagation. *Daphnia magna* infected with *B. daphniae* n. g., n. sp. were collected from a natural population in a human-made shallow eutrophic pond in Heverlee, Belgium (Pond OM2, Abdij van 't Park, 50°51'48"N, 4°43'17"E).

Corresponding Author: D. Refardt, Theoretical biology, ETH Zürich, Univesitätsstrasse 16, 8092 Zürich, Switzerland—Telephone number: +41 44 633 60 33; FAX number: +41 44 632 12 71; e-mail: dominik.refardt@gmail.com

¹Authors' contribution: D.R. initiated and coordinated the study and provided and interpreted molecular phylogeny and infection experiments data. J.V. provided and interpreted structural data. E.D. provided microsporidian samples and provided and interpreted infection experiments and field survey data. P.T.J.J. provided microsporidian samples.

Table 1. List of all microsporidian parasites that have been used in the phylogenetic analysis. Names of those species whose sequences have been obtained in this study are set in bold font. Note that origin of DNA sample does not necessarily give the location of the type specimen.

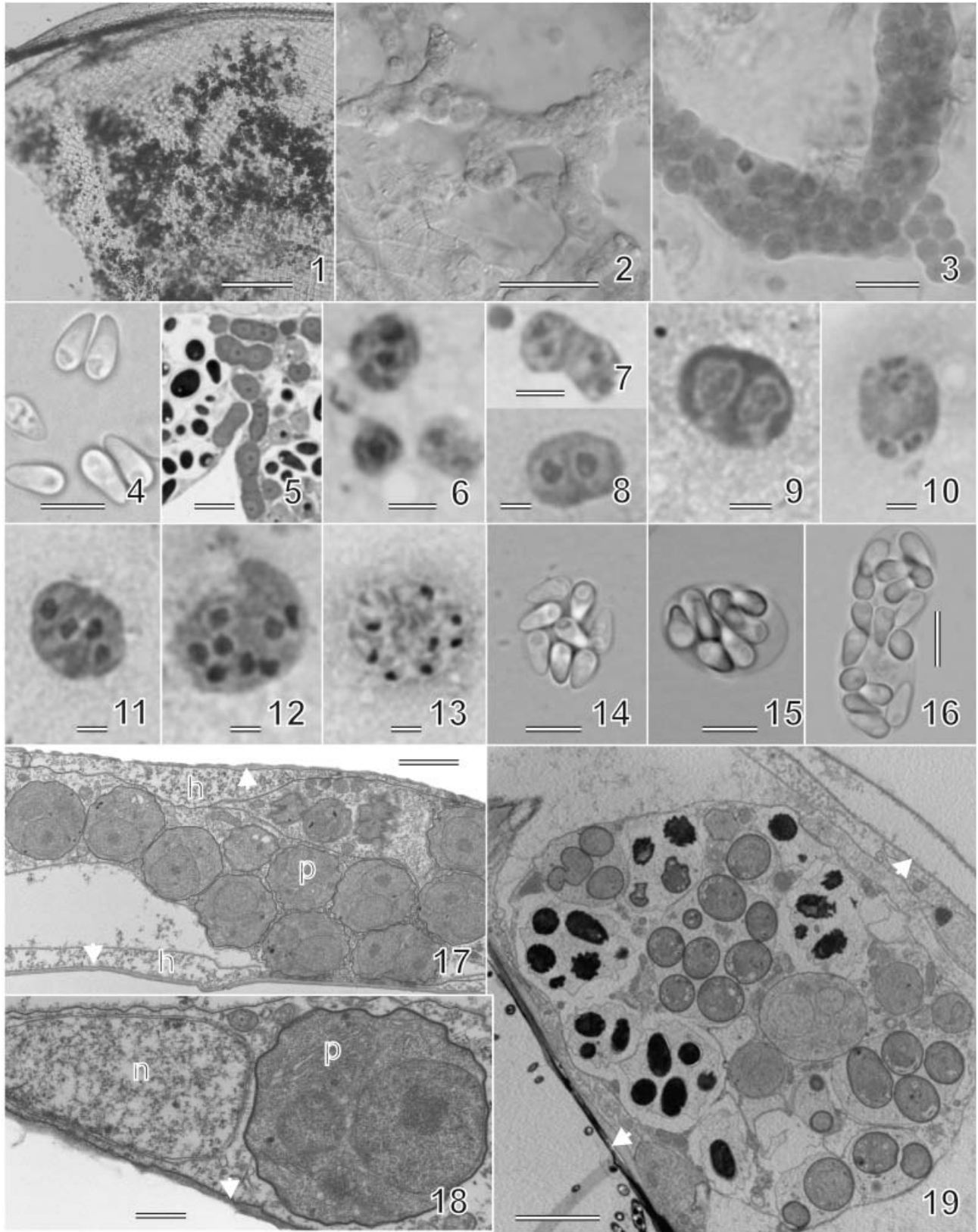
Parasite species	Host species	Infected tissue	GenBank accession no.	Species description	Origin of DNA sample
<i>Gurleya vavrai</i>	<i>Daphnia pulex</i> and <i>D. longispina</i>	Epidermis	AF394526	Green (1974)	Tärminne archipelago, Finland
<i>Gurleya daphniae</i>	<i>D. pulex</i>	Epidermis	AF439320	Friedrich et al. (1996)	Graz, Austria ^a
<i>Microsporidium</i> sp. "Lake George"	<i>D. mendotae</i>		EU075353		Lake George, Columbia County, WI, USA (43°31'20"N, 89°22'52"W)
<i>Microsporidium</i> sp. "Ångskärs-klubben 115/117"	<i>D. longispina</i>		EU075351		Hällnäs peninsula, Northeastern Uppland, Sweden (60°30'02"N, 18°04'30"E) (see Bengtsson and Ebert 1998)
<i>Microsporidium</i> sp. "Ångskärs-klubben 126"	<i>D. longispina</i>		EU075352		
<i>Binucleata daphniae</i>	<i>D. magna</i>	Epidermis	EU075347		OM2, Abdij van 't Park, Heverlee, Belgium (50°51'48"N, 4°43'17"E) ^a
<i>Senoma globulifera</i>	<i>Anopheles messeae</i>	Midgut epithelium	DQ641245	Simakova et al. (2005)	Tomsk region, Western Siberia ^a
<i>Microsporidium</i> sp. "Turtle lake"	<i>D. pulicaria</i>	Epidermis	EU075357		Turtle lake, Walworth County, WI, USA (42°43'37"N, 88°40'55"W)
<i>Microsporidium</i> sp. "Ripley Lake I"	<i>D. pulicaria</i>	Epidermis	EU075355		Lake Ripley, Jefferson County, WI, USA (43°00'09"N, 88°59'36"W)
<i>Microsporidium</i> sp. "Ripley Lake II"	<i>D. pulicaria</i>	Epidermis	EU075356		
<i>Microsporidium</i> sp. "Ångskär 16"	<i>D. pulex</i>		EU075349		Hällnäs peninsula, Northeastern Uppland, Sweden (60°28'53"N, 18°04'15"E) (see Bengtsson and Ebert 1998)
<i>Microsporidium</i> sp. "Ångskär 21"	<i>D. longispina</i>		EU075350		
<i>Berwaldia schaefernai</i>	<i>D. galeata</i>	Ovaries, fat body and more	AY090042	Vávra and Larsson (1994)	Pond Velky Palenec near the town of Blatna Czech Republic (49°25'29"N, 13°52'55"E) ^a
<i>Microsporidium</i> sp. "Fribourg"	<i>D. magna</i>		EU075348		Fribourg, Switzerland (46°47'30"N, 7°09'31"E)
<i>Larsonia obtuse</i>	<i>D. pulex</i>	fat cells, haemocytes	AF394527	Vidtman and Sokolova (1994)	Tvärminne archipelago, Finland
<i>Microsporidium</i> sp. "Lake Lulu"	<i>D. pulicaria</i>		EU075354		Lake Lulu, Walworth County, WI, USA (42°49'59"N, 88°26'58"W)
<i>Hazardia</i> sp.	<i>Anopheles crucians</i>		AY090066	Vossbrinck et al. (2004)	
<i>Hazardia milleri</i>	<i>Culex quinquefasciatus</i>		AY090067	Vossbrinck et al. (2004)	
<i>Marsoniella elegans</i>	<i>Cyclops vicinus</i>		AY090041	Vávra et al. (2005)	

^aType locality.

The parasite occurs both in this and in an adjacent pond (OM3). These ponds can be connected in winter when their water level is high. The ponds were used for carp culture and at present, a diverse fish community is present: mainly carp (*Cyprinus carpio*), Prussian carp (*Carassius gibelio*), perch (*Perca fluviatilis*), and

tench (*Tinca tinca*). The parasite has tentatively been named *Microsporidium* 2 in previous studies of this population (Decaestecker et al. 2003, 2004, 2005). The parasite was maintained in a clonal population of the host from which it was originally isolated (host genotype BE-OM2-41). *Daphnia* were kept in arti-

Fig. 1–19. Low-power view of the carapace of *Daphnia magna* adults infected with *Binucleata daphniae* n. g., n. sp. **1.** Heavily infected host with spores accumulated in the hemocoel of the carapace. Scale bar = 0.2 mm. **2.** Infected cells in the hemocoel form irregular strands in the early phase of infection. Nomarski phase-contrast. Scale bar = 50 µm. **3.** Round presporonts are a very frequently encountered life stage (compare with Fig. 17). Osmic acid impregnation. Scale bar = 10 µm. Fig. 4–16. Light microscope views of *B. daphniae*. Scale bar = 2.5 µm for Fig. 6–13, and 5 µm for Fig. 4, 5, 14–16. **4.** Spores (fresh on agar monolayer). **5.** Semithin section of infected host cell showing short chains of uninucleate dividing stages (compare with Fig. 21–23). Toluidine Blue staining. Fig. 6–13. Developmental stages in Giemsa-stained smears. **6.** Uninucleate meront and two binucleate cells of early presporonts, the most frequently observed life cycle stage. **7.** Dividing presporont. **8, 9.** Growing presporonts. Note that in Fig. 9 the presporont nuclei are preparing for karyokinesis. **10.** Early sporogony in which the sporont nuclei migrated to opposite parts of the cell and divided. **11.** Four-nucleate sporont. **12.** Final, eight nucleate sporont. **13.** Formation of spores in the sporont. **14.** Sporophorous vesicle (fresh). The thin wall of the sporophorous vesicle is almost invisible in transmitted light. **15.** Sporophorous vesicle visualized by Congo Red staining. **16.** Less frequent sporophorous vesicle with 16 spores. Note its characteristic elongate shape (Congo Red staining). Fig. 17–19. Low-power electron micrographs showing the location of *B. daphniae* in cells lining the internal surface of the carapace of *D. magna* or occurring in the carapace lumen. **17.** A group of presporonts (p) in a cell adhering to hypodermal cells (h) of the host. Arrowheads indicate host cuticle. Scale bar = 2 µm. **18.** Hypodermal cell (with its nucleus, n) of *D. magna* with one presporont cell (p) and the cuticle (arrowhead) of *B. daphniae*. Scale bar = 500 nm. **19.** A hypertrophied cell, filled with presporonts and various sporogonial stages, spanning the carapace lumen. Arrowheads indicate *D. magna* cuticle. Scale bar = 5 µm.



ficial medium (Ebert, Zschokke-Rohringer, and Carius 1998) under constant temperature ($20^{\circ}\text{C} \pm 1^{\circ}\text{C}$) and a 16:8 h light:dark cycle. Animals were fed 6×10^7 cells of the green alga *Scenedesmus* sp. every other day.

A further 10 isolates of other microsporidian parasites have been obtained from infected *Daphnia* stored in 70% ethanol and were only used for the construction of the molecular phylogeny (Table 1). Swedish and Swiss samples were kindly provided by J. Bengtsson (Swedish University of Agricultural Sciences, Uppsala, Sweden) and S. Lass (Center of Infectious Disease Dynamics, Penn State University, PA), respectively.

Light microscopy. Spore immobilization, photography, and Giemsa staining were performed according to methods described in Vávra and Maddox (1976). Fresh, agar-immobilized and fixed Giemsa-stained spores were measured on a computer screen using the Olympus M.I.S.Quick PHOTO MICRO program. Sporophorous vesicles were visualized by in vivo staining of squashed infected tissues with 1% (w/v) Congo Red. The following two archival Giemsa-stained smears of microsporidians infecting hypodermal tissues of *D. magna* were used for comparison: slide labeled *Nosema elongatum*, *D. magna*, Vrbno, and the slide labeled *Thelohania cladocera*, *D. magna*, Lohovec, 1935 (both slides belong to the slide collection of Otto Jírovec, Department of Parasitology, Faculty of Science, Charles University in Prague, Czech Republic).

Electron microscopy. Infected *Daphnia* were selected under low-power magnification of the light microscope and were fixed either for 1 h in 0.1 M phosphate buffer containing 1% (v/v) glutaraldehyde and 1% (w/v) OsO_4 (Hirsch and Fedorko 1968) or in phosphate buffer as above with 2.5% (v/v) glutaraldehyde followed by fixation in 1% (w/v) OsO_4 . During the first few minutes in the fixative, the animals were dissected and carapace samples were then dehydrated in a graded ethanol series and acetone and embedded in Polybed 812 epoxy resin. Ultrathin sections were stained with uranyl acetate and lead citrate and examined with a JEOL 1010 (JEOL, Tokyo, Japan) electron microscope equipped with a Megaview 3 CD camera (Olympus, Münster, Germany).

DNA extraction, amplification, and sequencing. Infected animals were stored in 70% ethanol and washed twice with distilled water before DNA extraction. DNA from whole animals was extracted following the protocol of Refardt and Ebert (2006). Primers 5'-CACCAGGTTGATTCTGCCTGAC-3' and 5'-GGTC CGTGTTC AAGACGGG-3' were used to amplify the 16S ribosomal RNA (rRNA) gene, internal transcribed spacer (ITS), and partial 23S rRNA gene following the protocol of Refardt et al. (2002). Sequencing was done by automated means by Synergene Biotech GmbH (Schlieren, Switzerland). Sequences were published in GenBank (for accession numbers see Table 1).

Phylogenetic analysis. We only used 16S rRNA gene sequences for phylogenetic reconstruction because ITS and 23S rRNA gene sequences were not available from all species that were included in the phylogeny. Sequences from eight other microsporidian species were downloaded from GenBank (Table 1). *Marssoniella elegans*, *Hazardia* sp., and *Hazardia milleri* were used as outgroup in the molecular phylogeny.

All sequences were automatically aligned with CLUSTAL W (Thompson, Higgins, and Gibson 1994) and edited by eye using BioEdit v5.0.9 (Hall 1999). Putative primer sites at the 3'- and 5'-ends were truncated and characters that could not be aligned unambiguously were removed, leaving an alignment of 1,260 bp length. Phylogenetic reconstruction was carried out with Bayesian inference (MrBayes v3.1.2, Ronquist and Huelsenbeck 2003) and maximum likelihood (PAUP* v4.0 β 10, Swofford 2003).

Bayesian inference. MrBayes was run for 100,000 generations using the GTR model with γ -distributed rate variation across sites and a proportion of invariable sites. Every 100th generation was sampled. The first 25% of samples was discarded as burn-in, parameter values were summarized, and a consensus tree was constructed. Standard deviation of split frequencies, which estimates the precision of the clade probabilities, reached 0.009 after 100,000 generations.

Maximum likelihood. Likelihood settings (GTR+I+G) were selected by AIC in Modeltest 3.8 (Posada and Crandall 1998). Tree search in PAUP* was done heuristically with random stepwise addition (10 replicates) and TBR branch swapping. A majority-rule consensus tree was calculated from 100 bootstrap replicates.

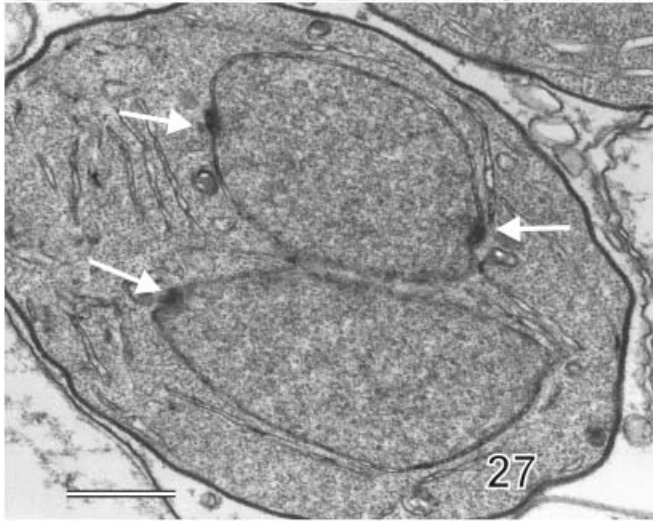
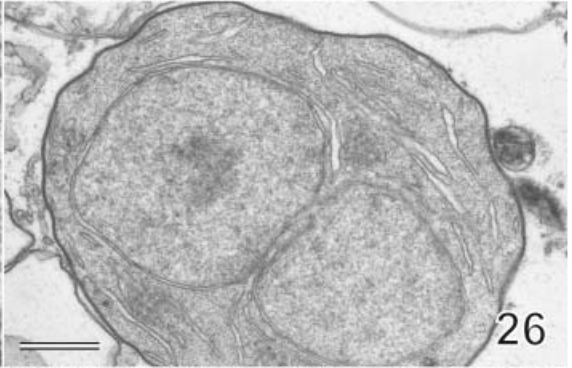
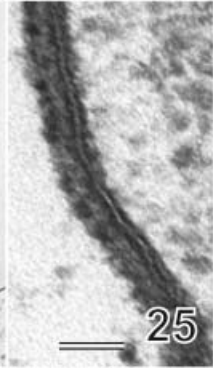
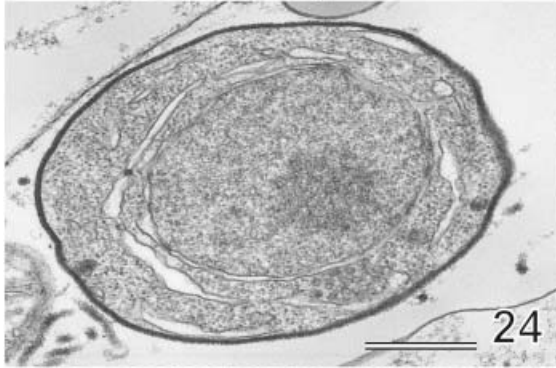
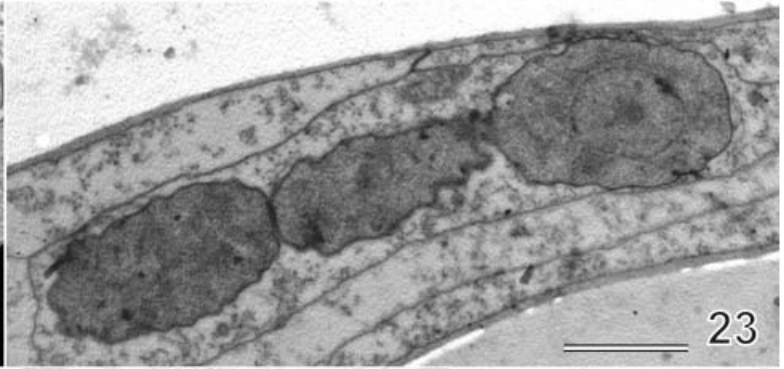
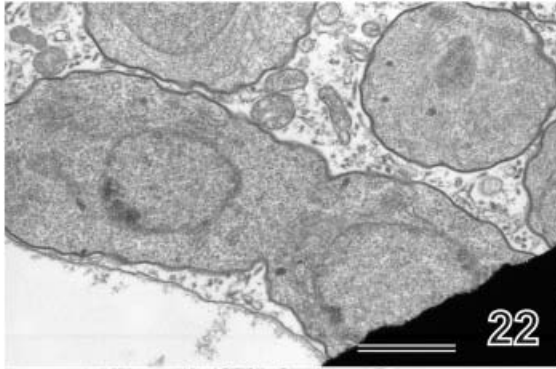
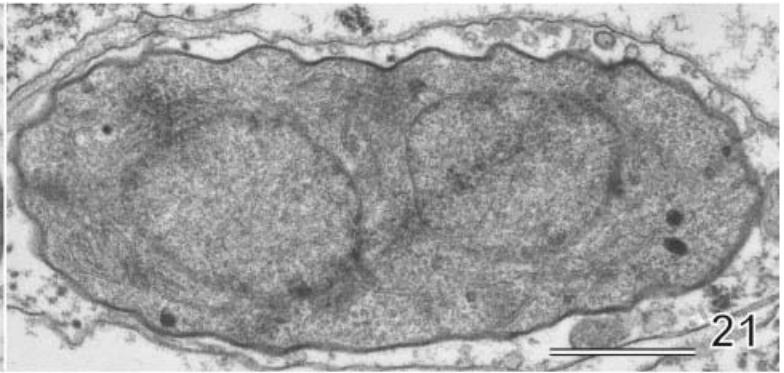
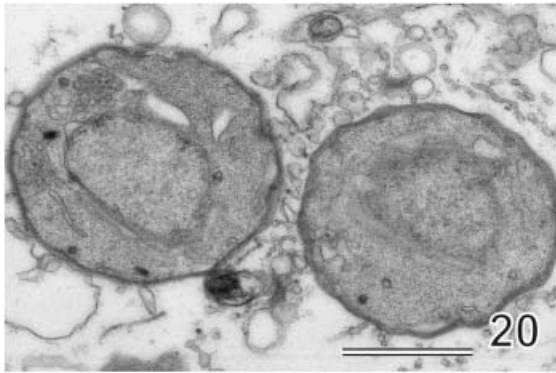
Field study. We studied the population dynamics of *B. daphniae* and its host *D. magna* in the ponds OM2 and OM3 in Heverlee, Belgium. From April through December in 1999 and in 2000, we collected *D. magna* samples at weekly or two-weekly intervals (interval time inversely related to water temperature) with a 200- μm plankton net. Samples were kept at 4°C until analysis. To determine density of *D. magna*, we took quantitative samples. In each pond, at three different locations in the vicinity of a fixed sample station, we took five samples of 1-L volume. All samples were sampled throughout the whole water column. Different sampling material was used for each pond and sterilized between sampling dates. Live samples were screened for the presence of *B. daphniae* with light from the top and through the bottom. Infections are clearly visible as infected animals appear opaque in incident light.

Experiments addressing transmission, persistence, and virulence of *Binucleata daphniae* n. g., n. sp.

Vertical transmission. To investigate whether *B. daphniae* shows vertical transmission from mother to offspring, nine separate stock cultures were set up from infected *Daphnia*, isolated from a field population (OM2, Abdij van 't Park, Heverlee). This coincides with nine cultures of different *B. daphniae* isolates, as parasites picked up by individual *Daphnia* can be considered to be different isolates (Carius, Little, and Ebert 2001). From each *Daphnia* stock culture, we isolated five mothers that were individually raised and from which two juveniles of the first clutch were removed at maximum 24 h after birth and checked for infection after 30 days. Every 3 days, animals were transferred into fresh medium and newborns were removed. Mothers and juveniles were individually raised in 60-ml beakers and fed every 2 days with 4.8×10^6 algal cells.

Parasite persistence in single-clone host populations. To address trans-generational persistence of *B. daphniae* in different genotypes of its host *D. magna*, small experimental populations

Fig. 20–28. Fine structure of *Binucleata daphniae* n. g., n. sp.: meronts, presporonts and early sporonts. 20. Uninucleate youngest meronts. Note the high density of the cytoplasm, the absence of endoplasmic reticulum, and other vesicular structures of the cell. The plasma membrane is covered with a diffuse, dense coat. Scale bar = 1 μm . 21–23. The division of uninucleate meronts (compare with Fig. 5). Scale bars for Fig. 21, 22 = 1 μm ; 23 = 2 μm . 24. Uninucleate cell at the meront/presporont transition with a relatively large nucleus, which will probably divide into two nuclei characterizing the presporonts. Membranous compartmentalization of the cytoplasm is more complex when compared with meronts. Scale bar = 500 nm. 25. Detail of the plasma membrane of the stage in Fig. 24 showing the thick dense coat. Scale bar = 50 nm. 26. The presporont has two, diplokaryon-like, however less intimately related nuclei. Cytoplasm contains ER lamellae and Golgi vesicles, plasma membrane is covered with dense coat. Scale bar = 500 nm. 27. The binucleate presporonts are still dividing as suggested by the appearance of spindle plaques at their nuclei (arrows). Scale bar = 500 nm. 28. Sporogony is marked by separation of the two nuclei of the presporont and by substantial increase of membranous and vesicular structures in the cytoplasm. Scale bar = 500 nm.



consisting of approximately 15 animals of a single host clone were set up in 100-ml beakers filled with medium. Twelve different host clones were used and replicated 3 times (36 total populations). Clones were isolated from natural populations in Cumnor (near Oxford, UK; clones C1–3), Heverlee (near Leuven, Belgium; H1–3), Kniphagen (near Plön, Germany; K1–3), and Laidy Kirk (80 km southeast of Edinburgh, UK; L1–3). These single-clone populations were exposed to 50,000 spores of *B. daphniae* (isolate from host genotype BE-OM2-41) each and maintained for six wk after which they were checked for infection. Populations were fed three times a week with 1.5×10^7 algal cells.

Virulence. Virulence was measured as the effect of *B. daphniae* on the fecundity and longevity of its host in nine *Daphnia* clones from three different populations (i.e. OM1, OM2 and OM3, Abdij van 't Park, Heverlee). Ten juveniles of the second brood of each clone were split in two groups of five juveniles each and transferred into 150-ml beakers. After two days, one group of each clone was exposed to 1.85×10^6 parasite spores obtained from tissue of infected *Daphnia*, while the other group as control received an equal amount of tissue from non-infected *Daphnia*. The groups were fed every other day with 1.2×10^7 algal cells. Newborns were removed and counted every three days when the groups were transferred into fresh medium. Infection rates, number of newborns per group, and mortality were scored after 40 days. Differences in fecundity and longevity were analyzed with non-parametric statistics using JMP v. 5.0.1a (SAS Institute Inc., Cary, NC).

In all experiments, individual *Daphnia* were checked visually for infection and, in cases of doubt, with a light microscope (phase contrast, 400X magnification).

RESULTS

Light microscopy. *Daphnia* heavily infected with *B. daphniae* n. g., n. sp. appeared opaque in incident light. Low-power microscope examination of infected *Daphnia* revealed spores accumulating inside cells on the internal carapace surface and in cells lining the hemocoelic space inside the postabdomen. Some infected cells and free spores were observed floating in the host's hemocoel (Fig. 1). Early during infection, when spores had not yet developed, irregular, ribbon-like formations in the carapace were discernible, representing host cells with early developmental stages of the parasite (Fig. 2, 3). Following death and decay of infected hosts, sporophorous vesicles (SPOVs) with spores and free spores from broken SPOVs were released spontaneously into the aquatic environment. Individual fresh spores were elongate pyriform, very slightly curved along their longitudinal axis, $4.9 \times 2.5 \mu\text{m}$ ($4.5\text{--}5.3 \times 2.3\text{--}2.7$, $n = 20$) in size (Fig. 4). Giemsa-stained spores were $3.9 \times 2.2 \mu\text{m}$ in size ($n = 20$) (Fig. 53).

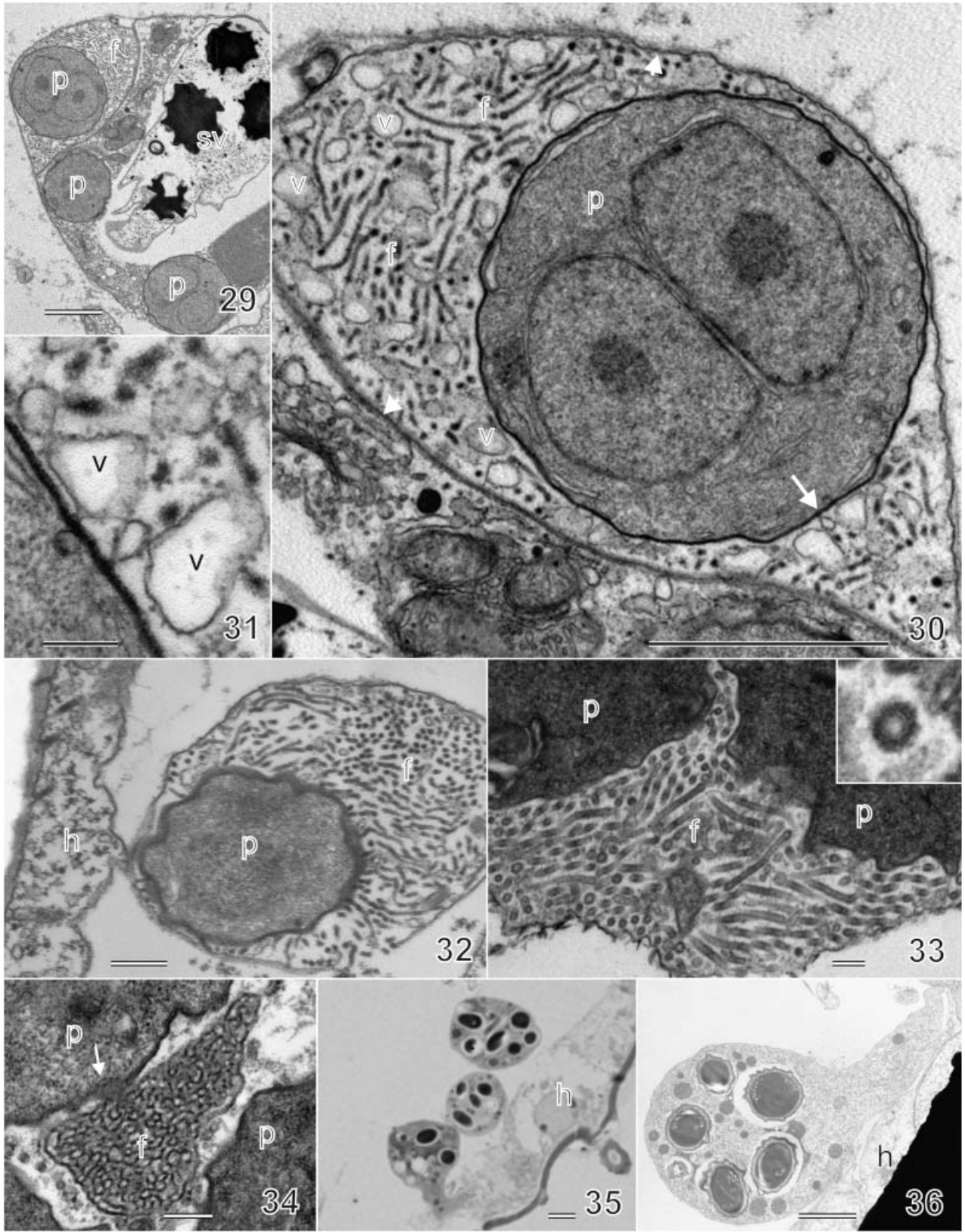
Upon squashing, developmental stages (DS) and spores within SPOVs were released from living animals (Fig. 6–16). On Giemsa-stained smears (Fig. 6–13) the DS appeared as short chains of cells with several nuclei (best seen in semithin sections, Fig. 5)

and larger, round uninucleate stages (Fig. 6). Both these stages were rarely observed. Most frequently encountered DS were round or oval binucleate cells around $4.0 \times 3.5 \mu\text{m}$ (Fig. 6–9), sometimes dividing by binary fission (Fig. 7), with both cell and nuclear size quite variable (Fig. 6, 8, 9). The nuclei of these binucleate stages migrated to the opposite pole of the cell and divided twice to form a cell with four and later eight nuclei (Fig. 10–12). Occasionally an additional karyokinesis occurred and a cell with 16 nuclei was formed (not shown). A spore was formed around each nucleus (Fig. 13). Immature spores had a large posterosome, staining magenta in the posterior part of the spore. Mature spores stained with Giemsa after acid hydrolysis showed one small nucleus in the spore (not shown). Fresh spore groups released by squashing of infected hosts were slightly oval, and 8–10 μm in size if there were eight spores in the cluster (Fig. 14, 15). Spore groups with 16 spores were usually elongate ellipsoid, $18 \times 6 \mu\text{m}$ in size (Fig. 16). Each spore group was surrounded by a very thin and rather inconspicuous SPOV membrane, nearly invisible (Fig. 14) unless stained with Congo Red (Fig. 15).

Electron microscopy.

Merogony and presporonts. The youngest DS found were round uninucleate meronts with dense cytoplasm and with very few endogenous membranes (Fig. 20). The meront plasma membrane was covered with a diffuse, structureless, dense coat about 10–20 nm thick. Numerous, blister-like expansions of the coat into the cytoplasm of the host cell were seen around the meronts. The meronts evidently divided or were products of a division. Dividing stages were elongate cells with two individual nuclei (Fig. 21), cells just seen when dividing (Fig. 22) or cells forming a short chain resulting from division (Fig. 23). The cell coat on dividing cells had the same character as described above. Presumably more advanced developmental stages were oval cells with a single large nucleus, and several cisternae of endoplasmic reticulum (ER) in their cytoplasm (Fig. 24). The plasma membrane of these cells was also covered by a dense coat, similar to meronts (Fig. 25). We term these cells presporont mother cells. Karyokinesis in these PMCs gave rise to oval cells with two nuclei in a diplokaryon-like configuration. We term these cells presporonts (PSPs). PSPs represent the most frequently found and characteristic stage after spores. PSPs were round to short oval with a quite regular outline. The twin nuclei in PSPs seemed not as tightly adhering as in a typical diplokaryon. The cytoplasm of the PSPs was moderately dense due to the presence of a number of ribosomes, and contained several cisternae of the ER and several areas of Golgi vesicles (Fig. 17, 18, 26, 29, 30, 42). The plasma membrane of the PSPs was covered with a dense coat, similar to earlier developmental stages. The coat occasionally expanded in a halo of dense fibrillo-tubular threads, membranous vesicles, and meandering fibrillar formations filling the surrounding of the parasite and forming a meshwork around its cell (Fig. 29–34). The threads were about 40 nm thick, radiated perpendicularly from the parasite surface, and had a finely granular substructure (Fig. 32–34). Some threads had a hollow interior lined with a membrane making

Fig. 29–36. The interaction of presporonts of *Binucleata daphniae* n. g., n. sp. with the host cell. **29.** Low-power view of a cell containing three presporonts (p) and a sporophorous vesicle with sporoblasts (sv). One of the presporonts is surrounded by extensive fibrillar meshwork. (f). Scale bar = 2 μm . **30.** Detailed view of part of Fig. 29. The presporont (p) is enclosed in a membranous sac (former host cell membrane or abortive sporophorous vesicle membrane formed by the presporont?) (arrowheads), filled solely with fibrillar (f) and vesicular (v) expansions of the presporont cell coat. Arrow = see Fig. 31. Scale bar = 1 μm . **31.** Detail of Fig. 30 (site labeled by arrow) showing the formation of vesicles (v) from the cell coat. Scale bar = 200 nm. **32.** Another example of a vesicular formation (host cell or abortive sporophorous vesicle?) containing presporont cell (p) and demonstrating that the sporont coat sends fibrillar expansions (f) into the vesicle volume (h = host hypodermal cell). Scale bar = 500 nm. **33.** Two presporont cells (p) surrounded by tubular expansions (f) of their cell coat. Scale bar = 200 nm. **Inset.** High magnification of a 40-nm-thick tubule showing its hollow center surrounded by a membrane and the dense coat material. **34.** Meandering meshwork of the coat material expanded (at arrow) from the coat of a presporont (p). Scale bar = 200 nm. **35.** Hemocyte-like cells packed with spores occur in the hemocoel of infected hosts, some free, some loosely attached to hypodermal cells (h). Semithin section, Toluidine Blue staining. Scale bar = 10 μm . **36.** Hemocyte-like cell attached to the hypodermis (h). Note that the spores inside the cell show signs of structural damage. Scale bar = 2 μm .



their tubular structure evident (Fig. 33 and inset). The threads and vesicles appeared to be continuous with the coat on the plasma membrane and had the same electron density (Fig. 30–34). Although the PSPs were ready for sporogony, they were still able to divide. At several occasions, we observed larger cells, similar to PSPs, in which the nuclei showed signs of imminent karyokinesis (Fig. 27).

Early sporogony. The developmental stages succeeding the PSPs were early sporonts (ESs), slightly elongate cells of less regular outline, in which the twin nuclei started to separate and the cytoplasm of which was more transparent, showing more ER cisternae and cytoplasmic vesicles (Fig. 28). During further development ESs elongated (Fig. 37–39). Their cytoplasm contained numerous ER cisternae and vesicles, and their nuclei were in some cases located at the opposite poles of the cell (Fig. 38). The SPOV membrane in the form of a thin, dense layer started to detach at some points from the surface of the sporont (Fig. 39, 40), resulting in a bi-layered structure of the formerly homogenous sporont coat (Fig. 41).

Late sporogony and spore formation. Late sporogony was marked by the formation of the SPOV enveloping the sporont as a sachet. The SPOV wall consisted of a single, structureless, 12-nm-thick layer of dense material (Fig. 40–44). The sporont started to divide inside the SPOV, forming sequentially two, four, and finally eight (less frequently 16) petal-like formations joined together at their base (Fig. 42, 43). Each cell of the parasite resulting from the division of the sporont had the nuclei at the distal pole of the “petal” and its cytoplasm had many ER cisternae and vesicles. Several double membrane vesicles, presumably representing mitosomes (Williams et al. 2008) were also present in each cell. The sporont cell was enveloped by a trilaminar structure represented by plasma membrane, a gap, and a dense coat (Fig. 44). Small granules and threads were scattered in the episporontal space around the dividing sporont (Fig. 42, 43, 45).

The division of the sporont eventually gave rise to individual sporoblast mother cells, each of which possessed a single large nucleus, and well-developed ER system (Fig. 45). These cells differentiated into sporoblasts, which are dense cells with an irregular outline and no visible cytoplasmic details (Fig. 29). Sporoblasts differentiated into pre-spore cells in which the coils of the future polar filament, its anchoring disk and polaroplast membranes started to form (Fig. 46). In young spores the polar filament had four thick and four thin coils. The polaroplast of immature spores consisted of irregular lacunae; the large nucleus was situated just below the polaroplast. The central part of the young spore was occupied by a large, round body, delimited by several membranes, filled with finely granular and sometimes dense material (Fig. 47, 48). This structure was already present in pre-spore cells. It originated probably as a Golgi product, but its function is unknown (Fig. 43). The posterior pole of the immature spore contained a vacuolar space with some Golgi membranes, leftovers from polar filament forming material. This was the primordium of the future posterior vacuole. Mature spores were encased by a 100-nm-thick endospore and a relatively thin (30 nm), single-layered exospore. The polaroplast was lamellar in structure (with 30–

40 nm spaced lamellae in mature spores, Fig. 51) and the polar filament had typically four (3–5) thick (200 nm) and typically four (3–5) thinner (130 nm) coils (Fig. 49, 50).

Location of infection. The infection by *B. daphniae* was limited to the carapace and postabdomen of the host *D. magna*. Examination of semithin and thin sections revealed the developmental stages and spores of the parasite in the epidermal cells lining the internal face of the two cuticular layers of the carapace. This is possible because the carapace of *Daphnia* consists of a layer of integument folded back on itself, producing a double layer enclosing a narrow hemocoelic space (Halcrow 1976). The cells of the external layer were significantly more infected. Some infected cells also adhered to the cells lining the carapace cavity and to the cells subtending the cuticle in the postabdomen of *D. magna*.

Molecular phylogeny. We amplified and sequenced the 16S rRNA gene, ITS, and partial 23S rRNA gene of *B. daphniae* and 10 other isolates of microsporidian parasites (Table 1). A BLAST search against GenBank as well as visual comparison of sequences in an alignment of microsporidian rRNA gene sequences found that they all belong to the “aquatic outgroup” (sensu Vossbrinck et al. 2004), a monophyletic sister group to parasites of mosquitoes, nested within the clade of microsporidia of freshwater origin (Vossbrinck and Debrunner-Vossbrinck 2005). Closely related species in the aquatic outgroup of which sequence data are available are *Berwaldia schaefermai*, *Gurleya daphniae*, *Gurleya vavrai*, *Larssonia obtusa* and *Senoma globulifera*. *Marssoniella elegans*, *Hazardia* sp., and *Hazardia milleri* also belong to the aquatic outgroup, but fall into a separate clade (Vossbrinck et al. 2004) and were therefore used as outgroup in the molecular phylogeny.

Bayesian inference and maximum likelihood methods gave identical results with most taxa bipartitions receiving high support values (Fig. 55). Three subgroups stood out, as they were clearly separated by long branches.

The closest relative of *B. daphniae* was found to be *S. globulifera* (Simakova et al. 2005). The 16S rRNA genes of the two sequences are 96.9%, ITS 81.0%, and partial 23S rRNA genes 92.7% identical.

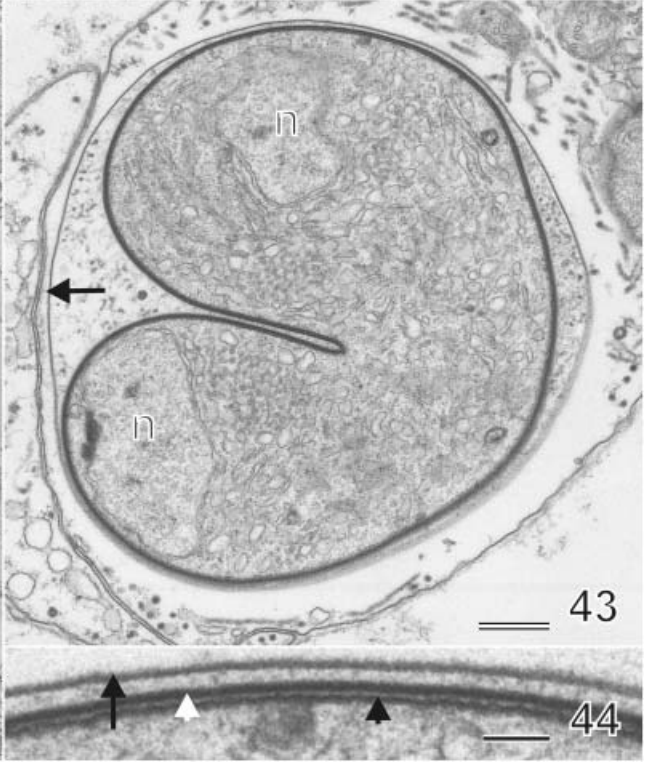
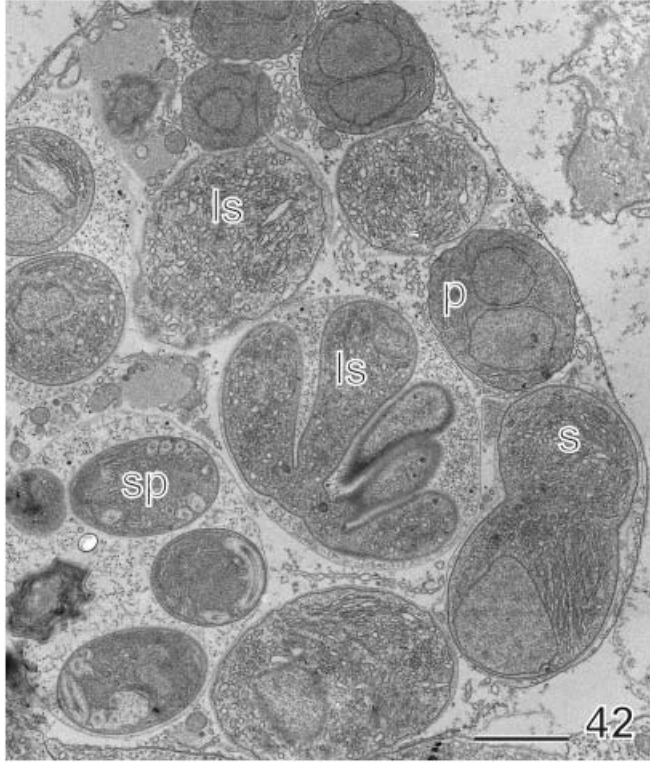
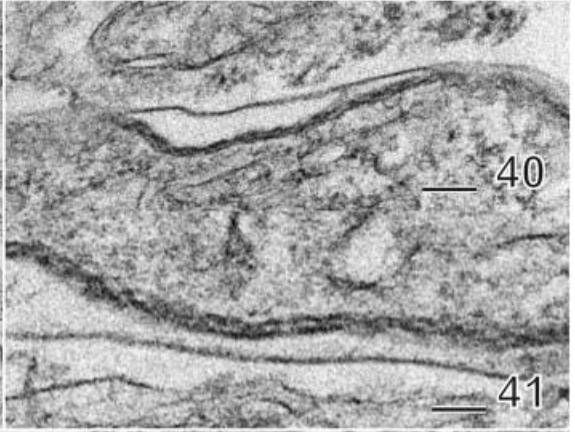
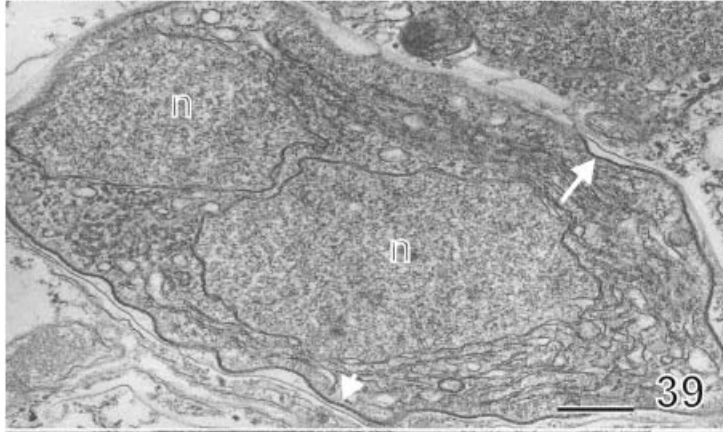
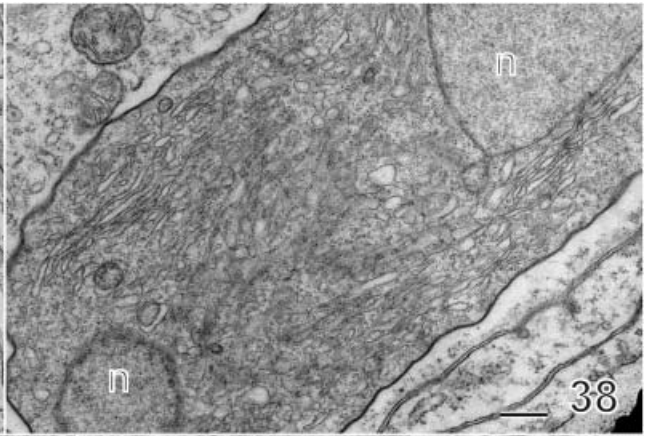
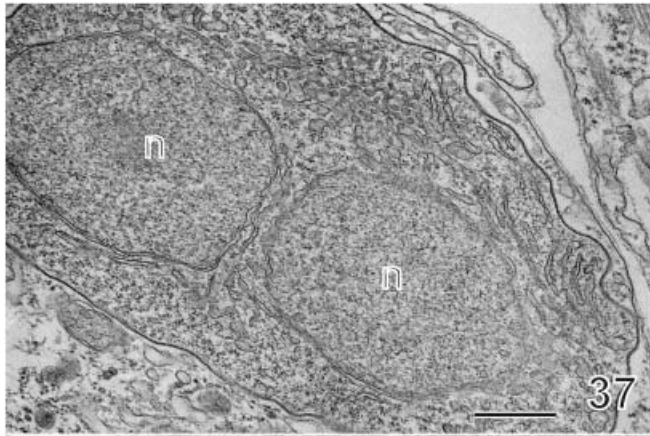
Field study. *Binucleata daphniae* occurred in both ponds in both years. Prevalence of infections showed a seasonal pattern that followed the density of the host *D. magna* and peaked in early summer, when up to 100% of the population were infected (Fig. 56). Population dynamics of *D. magna* showed a typical pattern that consisted of a period of very low abundance/absence during winter followed by a rapid increase and several density peaks during the growth season (Fig. 56).

Experiments addressing transmission, persistence and virulence of *Binucleata daphniae* n. g., n. sp.

Vertical transmission. An infected offspring was found in only one of the nine investigated *Daphnia* clones. In this clone, seven daughters survived, one of which was infected.

Parasite persistence in single-clone host populations. The parasite established persistent trans-generational infections in all replicate populations of all 12 host clones over 6 weeks (about three host generations). One replicate of clones C1 and C2 went extinct.

Fig. 37–44. Early sporogenesis of *Binucleata daphniae* n. g., n. sp. **37, 38.** Early sporont has a slightly undulating outline, its two nuclei (n) start to separate (final separation is seen in Fig. 38), cytoplasm is more transparent and has more membranous components in comparison with meronts. Scale bar = 500 nm. **39.** Early separation of the sporophorous vesicle membrane from the sporont coat is seen at arrow, site demonstrating changes occurring in the coat structure of the sporont is marked by arrowhead. Scale bar = 500 nm. **40.** Detail of Fig. 39 (arrow). Scale bar = 100 nm. **41.** Detail of Fig. 39 (arrowhead) showing the double-layered structure of the sporont cell coat. Scale bar = 50 nm. **42.** Host cell filled with different sporogenesis stages (p, presporont; s, sporont; ls, late sporont; sp, young spore). Scale bar = 2 μm. **43.** Finger-like division of a late sporont (n, nuclei; sporophorous vesicle membrane is at arrow). Scale bar = 500 nm. **44.** Detailed view of the sporophorous vesicle membrane (arrow) and of sporont cell membrane (black arrowhead) and its coat (white arrowhead). Scale bar = 100 nm.



Virulence. The parasite significantly reduced fecundity of its host (total number of newborns per group in parasite treatment = 153 ± 19 SE; in control = 214 ± 8 SE; Wilcoxon's matched-pairs test: $n = 9$, $P = 0.024$). There was a trend for reduction in longevity (percentage mortality per group in parasite treatment = $13\% \pm 5\%$ SE; in control = $0\% \pm 0\%$ SE; Wilcoxon's matched-pairs test: $n = 9$, $P = 0.068$).

DISCUSSION

Infected tissue. *Binucleata daphniae* n. g., n. sp. infected the carapace and postabdomen of *D. magna*. It seems that the infected cells originated in the hypodermis, but once infected were pushed away from the monolayer of tegumental cells. They were subsequently found adhering to the hypodermis and protruding into the hemocoel space inside the carapace. We speculate that the infection blocks apoptosis in infected cells that are sloughed off from the hypodermis. They remain viable and are replaced by uninfected cells. This allows the host to produce a new cuticle and continue to molt while infected. It has to be noted here that the cuticular pattern of the infected host is affected by the parasite: it is less regular than in uninfected individuals. The infection usually had a focal character and the cells lining the internal side of the carapace were never solidly packed with spores (e.g. like in *Daphnia pulex* infected with *G. daphniae*; see Fig. 4 in Friedrich et al. 1996).

We were unable to determine how *B. daphniae* spreads from the intestine of the host, the presumed site where the spores germinate after they have been ingested by filter feeding, into the epidermal cells of the tegument and how it then spreads from cell to cell. In the postabdomen of infected *Daphnia*, we observed cells resembling hemocytes that contained several individual spores, with each spore surrounded by a structureless halo, leading us to suppose that hemocytes carry the infection. Some spores appeared to be structurally intact, but others exhibited signs of structural damage (Fig. 35, 36). Developmental stages were not seen inside these hemocyte-like cells.

Fine structure of fibrillo-tubular and vesicular coat expansions recorded on several occasions around the presporonts (see Fig. 29–34) were difficult to interpret. The expansions protruded from the coat into the cytoplasm of the host cell and were seen in vicinity of host cell organelles. However, sometimes an extensive meshwork of coat expansions existed inside of a large vesicular formation limited by a membrane. Such vesicular formation was filled solely by coat expansions and there was no trace of host cell cytoplasmic organelles or their remnants. Such formations might represent either the situation in which only a membrane remained from the infected host cell, its cytoplasm replaced by the parasite structures (more probable alternative), or the formations might have been produced by the parasite. If the formation were of parasite origin, one might speculate that under some specific conditions the binucleate presporont forms a membrane around its cell (i.e. a precocious sporophorous vesicle). The coat expansions within the vesicle then would be homologous to secretory formations appearing in the episporontal space of many SPOV forming microsporidians. This hypothesis has to be verified. The coat pos-

sibly has an important function in the communication of the parasite with the host cell.

Phylogenetic position. We obtained sequence data from *B. daphniae* and 10 other microsporidian parasites of *Daphnia*. Although we have not collected any ultrastructural data on these additional species, we decided to include them in the molecular phylogeny because they were phylogenetically close to *B. daphniae* and additional information on geographical distribution, host species, and infected tissue provides insight into the importance of those characters for species differentiation and helps to better appreciate the phylogenetic position of *B. daphniae*.

All parasites that were sequenced in this study were found to belong to a clearly defined clade together with *B. schaefernai*, *G. daphniae*, *G. vavrai*, *L. obtusa*, and *S. globulifera* (Fig. 55) that has been termed the ‘‘aquatic outgroup’’ (Vossbrinck et al. 2004). The founder of this clade probably had a complex life cycle because microsporidians in sister clades have predominantly complex life cycles and infections with *B. schaefernai*, *G. vavrai*, and *L. obtusa* cannot be maintained in *Daphnia* in the laboratory (Refardt et al. 2002; Vávra 1964). The spontaneous occurrence of *Microsporidium* sp. ‘‘Fribourg’’ in an experimental outdoor population of *D. magna* at the University of Fribourg, Switzerland, suggests an airborne vector (*S. Lass*, pers. commun.). The absence of any natural populations of *D. magna* nearby suggests that this event was an opportunistic infection.

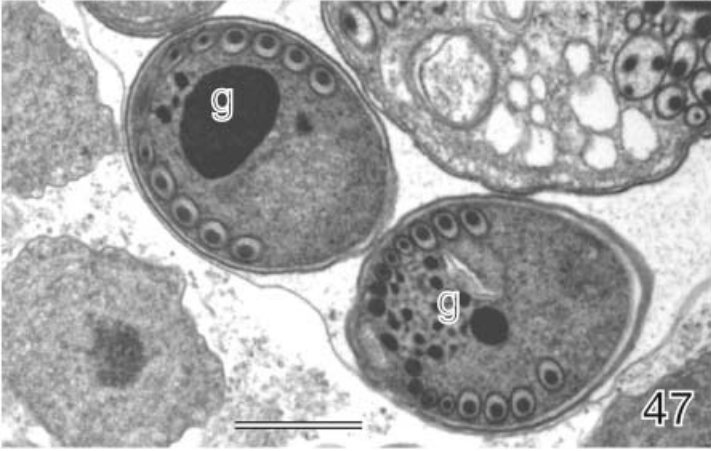
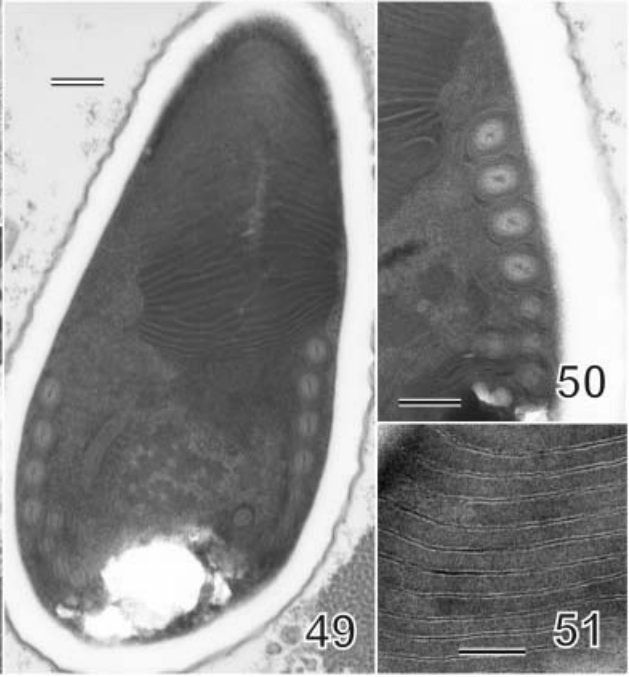
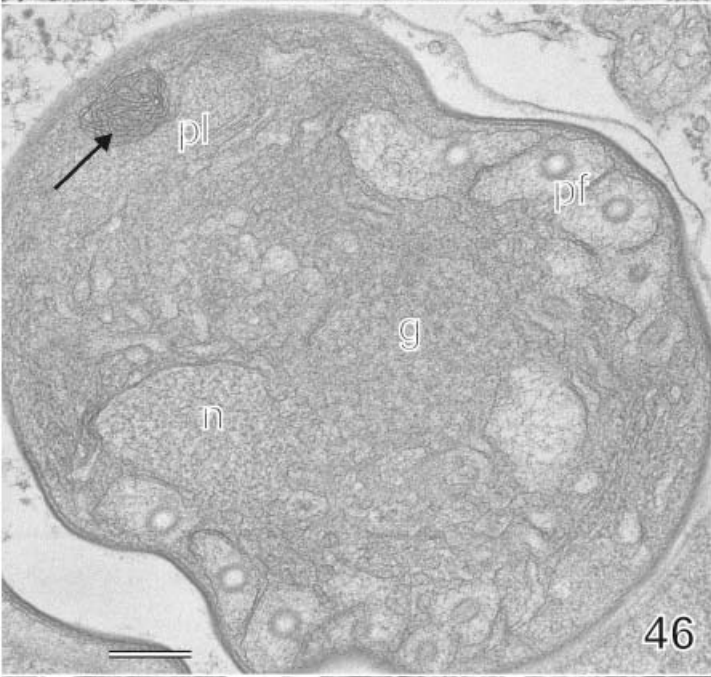
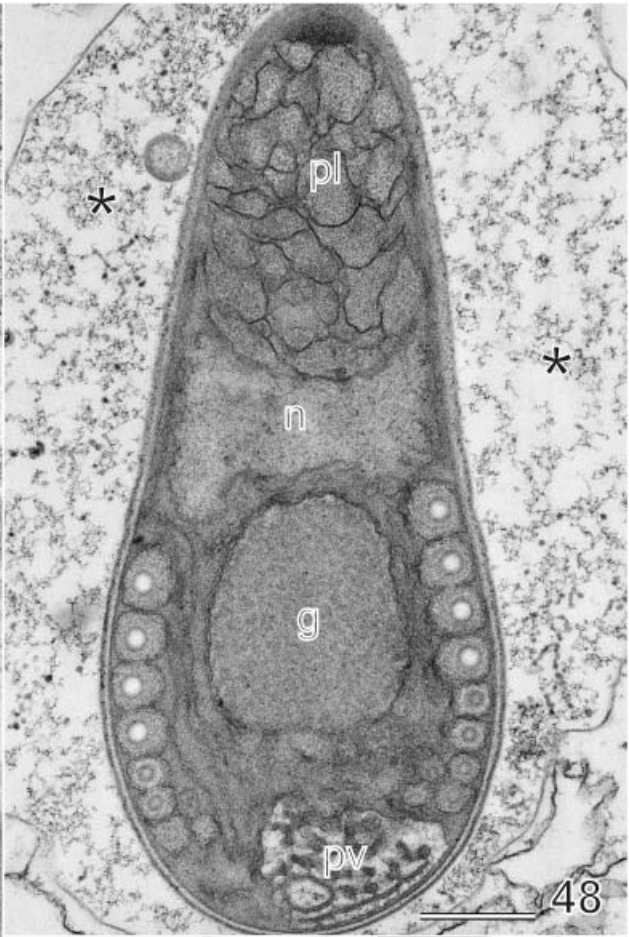
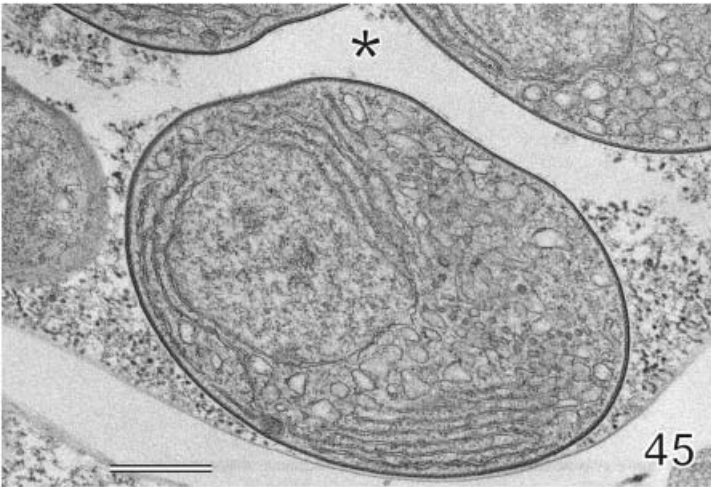
Tissue specificity seems to be rather conserved within the groups of this clade. Members of group 1 infect internal structures of their host and members of the other two groups are epidermal parasites. All parasites (with the exception of *S. globulifera*) infect *Daphnia*, yet the pattern of infected host species does not match the parasite phylogeny. The geographic origin of the samples does not reveal a pattern with simple interpretation either.

Binucleata daphniae n. g., n. sp. is the only microsporidian in this clade that has been shown to establish a persistent infection over several generations in its *Daphnia* host. We suggest that this parasite either has a single host life cycle or uses a second alternate host only facultatively. Interestingly, its closest relative is *S. globulifera*, a parasite of the midgut epithelium of *Anopheles messeae* (Simakova et al. 2005). The occurrence of a mosquito parasite amid these *Daphnia* parasites is intriguing and again supports the view that these parasites have mostly complex life cycles, possibly involving a cladoceran host and a mosquito. The infection of *S. globulifera* is asymptomatic (Simakova et al. 2005), which may explain why this is the only parasite in this group that has been found in a mosquito host until now.

Ecology. *Binucleata daphniae* has a simple life cycle with a direct and mainly horizontal transmission. Based on our results we cannot exclude vertical transmission of the parasite. However, we assume that the single infected newborn in the vertical transmission was probably horizontally infected very early in its life.

Our infection experiments show that *B. daphniae* lacks host genotype specificity and was able to infect all *D. magna* clones that were used in this study. The parasite established persistent infections over three host generations in 12 clones that represent a sample with presumably large genetic variation (Refardt and

Fig. 45–51. Late sporogonial stages of *Binucleata daphniae* n. g., n. sp. 45. Sporoblast mother cell surrounded by thin granular secretory material of the episporontal space (*). Sporophorous vesicle membrane is at arrowhead. Scale bar = 500 nm. 46. Sporoblast changing into a spore. The primordia of the thick and thin polar filament coils are visible (pf), as well as the germ of the polar filament anchoring disk (arrow) and the membranes of the future polaroplast (pl). Golgi material occupies central volume of the cell (g) together with the nucleus (n). Scale bar = 200 nm. 47. Young spores showing the dense Golgi-produced material (g) filling the core of the polar filament and forming a large central inclusion, which will disappear in the mature spore. Scale bar = 1 μ m. 48. More advanced young spore with the polar filament in its nearly mature form (n, nucleus; pl, polaroplast; g, Golgi material; pv, posterior vacuole). Secretory material in the episporontal space is at asterisk. Scale bar = 500 nm. 49. Mature spore. Scale bar = 200 nm. 50. Part of a mature spore showing thick endospore, one-layer-thin exospore, four thicker and four thinner polar filament coils. Scale bar = 200 nm. 51. Spacing of polaroplast lamellae in mature spore. Scale bar = 100 nm.



Ebert 2007). Our results confirm a previous study where 19 genotypes of *D. magna* from the same pond were found to be susceptible to *B. daphniae* (Decaestecker et al. 2003). This sets *B. daphniae* apart from other microparasites of *D. magna* that vary strongly in performance depending on the host genotype and/or show local adaptation to their host (Carius et al. 2001; Decaestecker et al. 2003; Ebert 1994, 2005; Ebert et al. 1998; Refardt and Ebert 2007). The parasite reduces *Daphnia* life-time fecundity and longevity by 10–50% both in the laboratory and in the field, yet when compared with other parasites, its impact on host fecundity was found to be comparatively low (this study; Decaestecker et al. 2003, 2005).

A survey of the population dynamics of both *B. daphniae* and its host in two natural populations of *D. magna* found that during winter, host populations have a very low density or even completely disappear. Because *B. daphniae* is very likely not vertically transmitted, this requires that the parasite overwinters as well and establishes new infections every year. Infections of *B. daphniae* occur as seasonal epidemics which peak at high prevalences in early summer (Fig. 56). *Daphnia* form resting stages in the form of diapausing eggs and when these hatch in spring, epidemics are probably initiated by grazing *Daphnia* that browse surface substrates and pick up infectious spores from the bottom of the pond early in the season (Ebert 2005). Infectious spores of *B. daphniae* have been recovered from up to 10-year-old sediment layers, which presumably allow the parasite to survive periods of low host abundance (Decaestecker et al. 2004).

Microsporidians exhibit a variety of transmission strategies that include both vertical and horizontal transmission in combination with life cycles of different complexity. It has been suggested that ecological conditions direct the adaptive evolution of these life cycles such that the current transmission strategy optimizes parasite fitness (Andreadis 2005). We propose that the characters mentioned above, i.e. a broad range of susceptible host genotypes, efficient transmission, long-lived spores, and moderately low virulence, allowed *B. daphniae* to abbreviate a previously complex life-cycle. These characters may also have further evolved in response to this life-cycle change, e.g. the parasite may have become more/less virulent following the change in its life-cycle.

Parasite identity and justification of new genus and species designations. Cladoceran crustaceans host more than 40 microsporidian species (Larsson and Voronin 2000). Long-term field and

laboratory observations indicated that these parasites are highly host- and tissue-specific (Ebert 1994, 2005; Green 1974; Stirnadel and Ebert 1997; JV., unpubl. data). This specificity even lead to the proposition that different microsporidians might be used as an aid in the classification of their hosts (Voronin 1995). Therefore, we can reasonably restrict discussion of the identity of *B. daphniae* to microsporidian parasites of *D. magna* (nine species) and specifically to hypodermal parasites (four species).

These four microsporidians that parasitize hypodermal tissues of *D. magna* are *N. elongatum* (Moniez 1887) Jirovec, 1936 (= *Microsporidium elongatum* in Larsson and Voronin 2000), *Agglomerata cladocera* (Pfeiffer 1895) Larsson, Ebert, and Vávra, 1996 (= *Telohonia cladocera* in Jirovec 1936), *Agglomerata volgensis* Larsson and Voronin, 2000, and *Flabelliforma magnivora* Larsson et al. 1998.

The description of *N. elongatum* belongs to the early history of the study of Microsporidia. Type slides do not exist and the original description does not allow proper identification of the parasite and its host. However, Giemsa-stained slides exist of the material which Jirovec (1936) used for species redescription. By comparing them with our material, we find that *B. daphniae* differs from *N. elongatum*. The latter has larger ($4.2 \times 2.5 \mu\text{m}$, $n = 20$) and more oval spores (cf. Fig. 52, 53).

The ultrastructure of *A. cladocera*, *A. volgensis*, and *F. magnivora* has been studied by Larson et al. (1996), Larsson and Voronin (2000), and Larsson et al. (1998), respectively. They differ from *B. daphniae* in many respects. Most importantly, both genera *Agglomerata* and *Flabelliforma* have isolated nuclei in all developmental stages and their presporogonial stages do not have the dense coat on the plasma membrane that is present in *B. daphniae*. *Agglomerata cladocera* bears bristle-like fibrils on the exospore, has a polar filament with a different thick/thin coils ratio, and has smaller spores (Larsson et al. 1996). Giemsa-stained spores of *A. cladocera* on the syntype slide made by Jirovec (slide labeled *T. cladocera*, *D. magna*, Lohovec, 1935) differ in shape and size ($3.3 \times 1.8 \mu\text{m}$) from spores of *B. daphniae* (cf. Fig. 53, 54). The spores of *A. volgensis* are distinctly different from the spores of *B. daphniae* in respect of a more pointed anterior pole, smaller size and different thick/thin polar filament coils ratio (Larsson and Voronin 2000). *Flabelliforma magnivora* has spores similar in shape and size to *B. daphniae*, but the spores possess an isofilar polar filament with 14–17 coils (Larsson et al. 1998) and

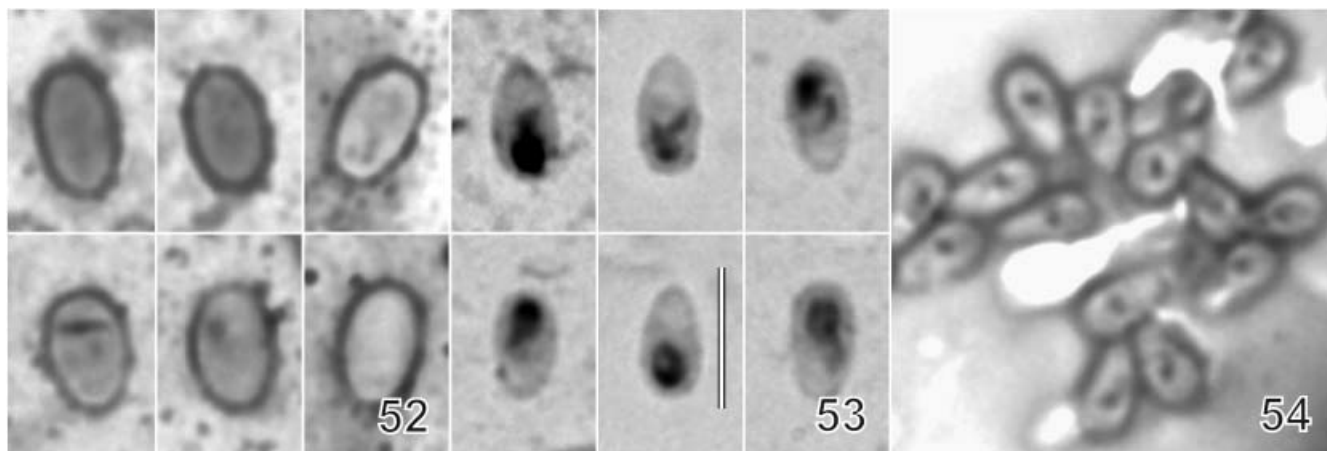


Fig. 52–54. Giemsa-stained spores of three microsporidian species infecting the hypodermal tissue of *Daphnia magna*. 52. *Nosema elongatum* (Moniez, 1887) Jirovec, 1936 (= *Microsporidium elongatum* in Larsson and Voronin 2000). 53. *Binucleata daphniae* n. g., n. sp. 54. *Telohonia cladocera*, *D. magna*, Lohovec, 1935 = *Agglomerata cladocera* of Larsson et al. 1996). Slides for Fig. 52 and Fig. 54 from the collection of O. Jirovec. All figures at the same magnification, Scale bar = 5 μm .

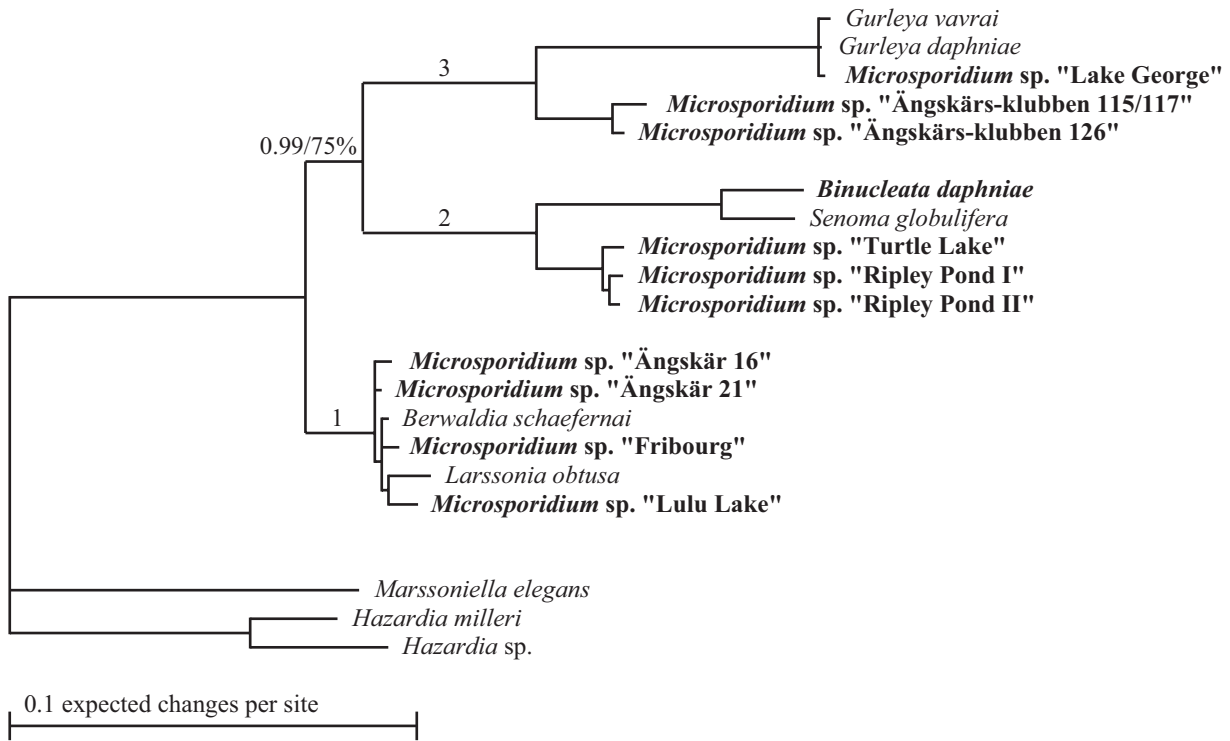


Fig. 55. Molecular phylogeny as obtained by Bayesian inference (BI) from an alignment of 16S rRNA genes of different microsporidian species. Maximum likelihood (ML) gave an identical topology. Species whose sequences were obtained in this study are set in bold font. Bold branches indicate taxa bipartitions which are supported by probabilities ≥ 0.99 (BI) and bootstrap values $\geq 99\%$ (ML). Numbers correspond to the grouping mentioned in the text. Support for the split between groups 2 and 3 is given as probability (BI) and bootstrap value (ML).

the two species are clearly separated phylogenetically (Refardt et al. 2002).

The microsporidian described here is not only different from the previously described microsporidians from Cladocera, its character states differ also from microsporidian genera listed in or published after the two most recent synopses of microsporidian genera (Canning and Vávra 2002; Larsson 1999). *Binucleata daphniae* is therefore described here as a new species to science and as a type species of a new microsporidian genus, defined mainly by two structural characters: (1) the coat on the plasma membrane already exists on meronts; and (2) the SPOV splits from this coat during sporogony. By definition, *B. daphniae* thus has the so-called merontogenetic sporophorous vesicle (Vávra and Larsson 1999). Few microsporidian genera (*Pleistophora*, *Trachipleistophora*, *Vavraia*) possess such a characteristic. In contrast to *B. daphniae*, the coat on the cells of representative members of these genera is much thicker and all of them form multisporous SPOV. The second conspicuous structural character of *B. daphniae* is the prevailing occurrence of binucleate cells amidst life cycle stages. The nuclei seem to be less tightly attached as in a typical microsporidial diplokaryon (e.g. those from terrestrial insects, like *Nosema bombycis*). However, in the absence of serial sections it is impossible to evaluate this character in full. Binucleate presporogonial stages occur in several microsporidians that infect Cladocera, three of them (*Gurleya*, *Berwaldia*, *Larssonsonia*) are phylogenetically closely related to *Binucleata* (Friedrich et al. 1996; Vávra and Larsson 1994; Vidtman and Sokolova 1994) (Fig. 55). *Binucleata daphniae* is the only genus and species in which such an association represents the prevailing life cycle stage. However, presently it is impossible to judge the evolutionary significance of the diplokaryotic nuclear configuration unless the ploidy of nuclei of microsporidians possess-

ing diplokarya is known. The two diplokaryon-like nuclei of *B. daphniae* may have resulted from a precocious nuclear division preceding sporogony.

Classification. None of the five different classification systems for microsporidia (Issi 1986; Sprague 1977; Sprague, Becnel, and Hazard 1992; Vossbrinck and Debrunner-Vossbrinck 2005; Weiser 1977) satisfies the requirement of harmonizing structural data conventionally used in microsporidia classification with molecular phylogeny relationships. This is the general situation in microsporidia, where synapomorphic structural data are not well defined. The best example is *Senoma globulifera*, a mosquito parasite, which, although phylogenetically the closest relative of *B. daphniae*, is structurally so dissimilar to *Binucleata*, that any conventional taxonomist would assign them at least into different families. If the relatively recent classification system of Sprague et al. (1992) is used, the occurrence of diplokaryon-like nuclei in *Binucleata* suggests its placement in the microsporidian class Dihaplophsea. Two orders exist in that class, according to the mode of nuclear dissociation, leading from the diplokaryotic to the uninucleate status. In the absence of proof that *Binucleata* possess meiosis, we place *Binucleata* only tentatively into the order Meiodihaplophsea Sprague et al. 1992. To select an appropriate family for *Binucleata* is also problematic. In fact, the Gurleyidae, the family containing *Gurleya* spp. from *Daphnia* which are phylogenetically close to *Binucleata*, is considered to be *incertae sedis* in the classification by Sprague et al. (1992). In other classification systems *Gurleya*-like microsporidians are placed either in the family Gurleyidae Sprague, 1977 or in the family Thelohaniidae Hazard & Oldacre, 1975. The second one seems to be a more appropriate ranking when the number of spores in the SPOV is considered and is used here.

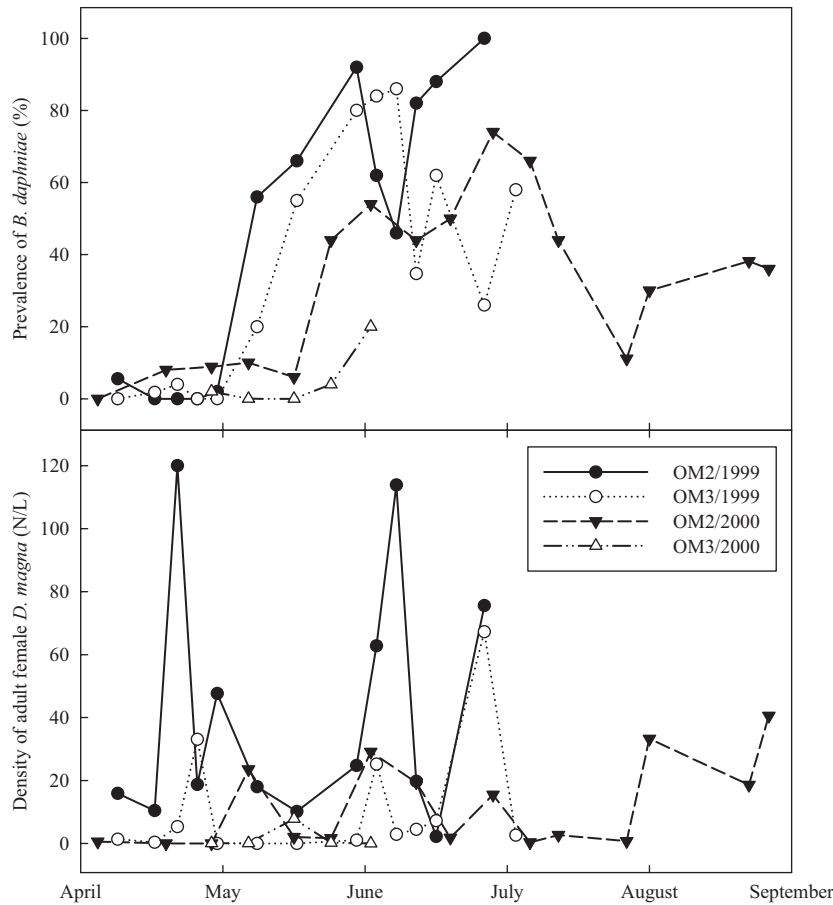


Fig. 56. **Upper panel:** seasonal prevalence of *Binucleata daphniae* n. g., n. sp. in two adjacent ponds (OM2 and OM3) in Heverlee, Belgium, over 2 yr. **Lower panel:** density of *Daphnia magna* in the same ponds during the same period.

Here, we include the phylum Microsporidia in the Kingdom Fungi, yet we do not adhere to the Botanical Code for the genus description because there is still discussion regarding whether the Microsporidia will be required to be described using the Botanical Code (Hibbett et al. 2007). In this we follow the general pattern used in recent descriptions of microsporidian taxa.

TAXONOMIC SUMMARY

Phylum Microsporidia Balbiani 1882
 Class Dihaplophasea Sprague et al., 1992
 Order Meiodihaplophasida Sprague et al., 1992, tentatively
 Family Thelohaniidae Hazzard and Oldacre 1975, tentatively
Binucleata n. g.

Diagnosis. All presporogonial stages (meronts to presporonts) have on their plasma membrane a dense, homogenous coat. The coat occasionally forms conspicuous tubulo-vesicular expansions protruding into the host cell cytoplasm. Meronts are uni and binucleate, at the transition between merogony and sporogony a round binucleate stage is formed, termed a presporont, representing the prevailing life-cycle stage. Presporonts divide in finger-like fashion into eight or 16 uninucleate cells maturing into spores enclosed in a thin-walled merontogenetic sporophorous vesicle the membrane of which originates by splitting of the presporont plasma membrane coat.

Etymology. Named after the prevailing binucleate life-cycle stage.

***Binucleata daphniae* n. sp.**

Diagnosis. As for the genus, the cell coat is about 10–20 nm thick, coat expansions in the form of vesicles, meandering expansions or tubules 40 nm thick and several micrometer in length. Spores are pyriform, 4.9 × 2.5 μm fresh, 3.9 × 2.2 μm when Giemsa-stained. Sporophorous vesicles round to oval (fresh: 10 × 8–10 μm when with eight spores and 18 × 6 μm when with 16 spores). Spores have lamellar polaroplast, anisofilar polar filament with four thick and four thin coils. Endospore is 100 nm thick, exospore is single-layered, 30 nm thick. Spores are without mucous coat. Infections occur in the integumental cells lining the hemocoel cavity of the carapace and of the postabdomen of *D. magna* Straus. Spores are autoinfective.

Type habitat. Shallow, eutrophic pond in Abdij van 't Park, Heverlee, Belgium (50°51'48"N, 4°43'17"E).

Type host. *Daphnia magna* Straus.

Type material deposition. Type slides are deposited in the International Protozoan Type Slide Collection, Department of Invertebrate Zoology, National Museum of Natural History, Smithsonian Institution, Washington, DC, USA, Account Nos. USNM (USNM Nos.1113093,1113094) and in the slide collection of Jiří Vávra at the Department of Parasitology, Faculty of Science, Charles University, Prague, Czech Republic.

Etymology. Named after the type host in which this species was found.

Gene sequences. Sequences of the 16S rRNA gene, ITS, and a portion of the 23S rRNA gene are deposited as GenBank Accession No. EU075347.

ACKNOWLEDGMENTS

Above all, we thank Dr. Kevin Halcrow (Department of Biology, University of New Brunswick, Saint John, NB Canada) for help in the identification of infected tissue. We also thank E. Kirchmannová for expert help in electron microscopy, A. Cappan, D. Ebert, and J. Hottinger for assistance with *Daphnia* cultures, and J. Bengtsson and S. Lass for the collection of parasite samples. This research was supported by the Swiss National Science Foundation to D.R., the FWO-Vlaanderen to E.D., and the Institute of Parasitology, ASCR (Research Project No. Z60220518) and the Grant Agency of the Czech Republic (Research Grant No. 524/07/1003) to J.V.

LITERATURE CITED

- Andreadis, T. G. 2005. Evolutionary strategies and adaptations for survival between mosquito-parasitic microsporidia and their intermediate copepod hosts: a comparative examination of *Amblyospora connectius* and *Hyalinocysta chapmani* (Microsporidia: Amblyosporidae). *Folia Parasitol.*, **52**:23–35.
- Becnal, J. J., White, S. E. & Shapiro, A. M. 2005. Review of microsporidia–mosquito relationships: from the simple to the complex. *Folia Parasitol.*, **52**:41–50.
- Bengtsson, J. & Ebert, D. 1998. Distributions and impacts of microparasites on *Daphnia* in a rockpool metapopulation. *Oecologia*, **115**:213–221.
- Canning, E. U. & Vávra, J. 2002. Phylum microsporidia Balbiani, 1882. In: Lee, J. J., Leedale, G. F. & Bradbury, P. C. (ed.), *The Illustrated Guide to the Protozoa*. 2nd ed. Society of Protozoologists, Lawrence, KS. p. 39–126.
- Carius, H. J., Little, T. J. & Ebert, D. 2001. Genetic variation in a host–parasite association: potential for coevolution and frequency-dependent selection. *Evolution*, **55**:1136–1145.
- Decaestecker, E., Declerck, S., De Meester, L. & Ebert, D. 2005. Ecological implications of parasites in natural *Daphnia* populations. *Oecologia*, **144**:382–390.
- Decaestecker, E., Lefever, C., De Meester, L. & Ebert, D. 2004. Haunted by the past: evidence for dormant stage banks of microparasites and epibionts of *Daphnia*. *Limnol. Oceanogr.*, **49**:1355–1364.
- Decaestecker, E., Vergote, A., Ebert, D. & De Meester, L. 2003. Evidence for strong host clone–parasite species interactions in the *Daphnia* microparasite system. *Evolution*, **57**:784–792.
- Ebert, D. 1994. Virulence and local adaptation of a horizontally transmitted parasite. *Science*, **265**:1084–1086.
- Ebert, D. 2005. Ecology, Epidemiology, and Evolution of Parasitism in *Daphnia* [Internet]. National Library of Medicine, National Center for Biotechnology Information, Bethesda, MD.
- Ebert, D., Zschokke-Rohringer, C. D. & Carius, H. J. 1998. Within- and between-population variation for resistance of *Daphnia magna* to the bacterial endoparasite *Pasteuria ramosa*. *Proc. R. Soc. B*, **265**: 2127–2134.
- Fast, N. M., Logsdon, J. M. Jr. & Doolittle, W. F. 1999. Phylogenetic analysis of the TATA box binding protein (TBP) gene from *Nosema locustae*: evidence for a microsporidia–fungi relationship and spliceosomal intron loss. *Mol. Biol. Evol.*, **16**:1415–1419.
- Friedrich, C., Winder, O., Schaffler, K. & Reinthaler, F. F. 1996. Light and electron microscope study on *Gurleya daphniae* sp. nov. (Microspora, Gurleyidae), a parasite of *Daphnia pulex* (Crustacea, Phyllopoda). *Eur. J. Protistol.*, **32**:116–122.
- Green, J. 1974. Parasites and epibionts of Cladocera. *Trans. Zool. Soc. Lond.*, **32**:417–515.
- Halcrow, K. 1976. The fine structure of the carapace integument of *Daphnia magna* Straus (Crustacea Branchiopoda). *Cell Tissue Res.*, **169**:267–276.
- Hall, T. A. 1999. BioEdit: a user-friendly biological sequence alignment editor and analysis program for Windows 95/98/NT. *Nucleic Acids Symp. Ser.*, **41**:95–98.
- Hibbett, D. S., Binder, M., Bischoff, J. F., Blackwell, M., Cannon, P. F., Eriksson, O. E., Huhndorf, S., James, T., Kirk, P. M., Lücking, R., Thorsten Lumbsch, H., Lutzoni, F., Matheny, P. B., McLaughlin, D. J., Powell, M. J., Redhead, S., Schoch, C. L., Spatafora, J. W., Stalpers, J. A., Vilgalys, R., Aime, M. C., Aptroot, A., Bauer, R., Begerow, D., Benny, G. L., Castlebury, L. A., Crous, P. W., Dai, Y.-C., Gams, W., Geiser, D. M., Griffith, G. W., Gueidan, C., Hawksworth, D. L., Hestmark, G., Hosaka, K., Humber, R. A., Hyde, K. D., Ironside, J. E., Kõljalg, U., Kurtzman, C. P., Larsson, K.-H., Lichtwardt, R., Longcore, J., Miadlikowska, J., Miller, A., Moncalvo, J.-M., Mozley-Standridge, S., Oberwinkler, F., Parmasto, E., Reeb, V., Rogers, J. D., Roux, C., Ryvarden, L., Sampaio, J. P., Schüssler, A., Sugiyama, J., Thorn, R. G., Tibell, L., Untereiner, W. A., Walker, C., Wang, Z., Weir, A., Weiss, M., White, M. M., Winka, K., Yao, Y.-J. & Zhang, N. 2007. A higher-level phylogenetic classification of the Fungi. *Mycol. Res.*, **111**:509–547.
- Hirsch, J. G. & Fedorko, M. E. 1968. Ultrastructure of human leukocytes after simultaneous fixation with glutaraldehyde and osmium tetroxide and “postfixation” in uranyl acetate. *J. Cell Biol.*, **38**:615–627.
- Hirt, R. P., Logsdon, J. M., Healy, B., Dorey, M. W., Doolittle, W. F. & Embley, T. M. 1999. Microsporidia are related to Fungi: evidence from the largest subunit of RNA polymerase II and other proteins. *Proc. Natl. Acad. Sci. USA*, **96**:580–585.
- Issi, I. V. 1986. Microsporidia as a phylum of parasitic protozoa. In: Beyer, T. V. & Issi, I. V. (ed.), *Protozoology*. Vol. 10: Microsporidia. (Protozoologia: Mikrosporidii). Nauka, Leningrad. p. 6–136.
- James, T. Y., Kauff, F., Schoch, C. L., Matheny, P. B., Hofstetter, V., Cox, C. J., Celio, G., Gueidan, C., Fraker, E., Miadlikowska, J., Lumbsch, H. T., Rauhut, A., Reeb, V., Arnold, A. E., Amtoft, A., Stajich, J. E., Hosaka, K., Sung, G. H., Johnson, D., O'Rourke, B., Crockett, M., Binder, M., Curtis, J. M., Slot, J. C., Wang, Z., Wilson, A. W., Schüssler, A., Longcore, J. E., O'Donnell, K., Mozley-Standridge, S., Porter, D., Letcher, P. M., Powell, M. J., Taylor, J. W., White, M. M., Griffith, G. W., Davies, D. R., Humber, R. A., Morton, J. B., Sugiyama, J., Rossman, A. Y., Rogers, J. D., Pfister, D. H., Hewitt, D., Hansen, K., Hambleton, S., Shoemaker, R. A., Kohlmeyer, J., Volkmann-Kohlmeyer, B., Spotts, R. A., Serdani, M., Crous, P. W., Hughes, K. W., Matsuura, K., Langer, E., Langer, G., Untereiner, W. A., Lücking, R., Budel, B., Geiser, D. M., Aptroot, A., Diederich, P., Schmitt, I., Schultz, M., Yahr, R., Hibbett, D. S., Lutzoni, F., McLaughlin, D. J., Spatafora, J. W. & Vilgalys, R. 2006. Reconstructing the early evolution of Fungi using a six-gene phylogeny. *Nature*, **443**:818–822.
- Jírovec, O. 1936. Über einige in *Daphnia magna* parasitierende Mikrosporidien. *Zool. Anz.*, **116**:136–142.
- Keeling, P. J. 2003. Congruent evidence from alpha-tubulin and beta-tubulin gene phylogenies for a zygomycete origin of microsporidia. *Fung. Genet. Biol.*, **38**:298–309.
- Larsson, J. I. R. 1999. Identification of microsporidia. *Acta Protozool.*, **38**:161–197.
- Larsson, J. I. R. & Voronin, V. N. 2000. Light and electron microscopic study of *Agglomerata volgensae* n. sp. (Microspora: Dubosqiidae), a new microsporidian parasite of *Daphnia magna* (Crustacea: Daphniidae). *Eur. J. Protistol.*, **36**:89–99.
- Larsson, J. I. R., Ebert, D. & Vávra, J. 1996. Ultrastructural study of *Glugea cladocera* Pfeiffer, 1895, and transfer to the genus *Agglomerata* (Microspora, Dubosqiidae). *Eur. J. Protistol.*, **32**:412–422.
- Larsson, J. I. R., Ebert, D., Mangin, K. L. & Vávra, J. 1998. Ultrastructural study and description of *Flabelliforma magnivora* sp. n. (Microspora: Dubosqiidae), a microsporidian parasite of *Daphnia magna* (Crustacea: Cladocera: Daphniidae). *Acta Protozool.*, **37**:41–52.
- Liu, Y. J., Hodson, M. C. & Hall, B. D. 2006. Loss of the flagellum happened only once in the fungal lineage: phylogenetic structure of kingdom Fungi inferred from RNA polymerase II subunit genes. *BMC Evol. Biol.*, **6**:e74.
- Posada, D. & Crandall, K. A. 1998. Modeltest: testing the model of DNA substitution. *Bioinformatics*, **14**:817–818.
- Refardt, D. & Ebert, D. 2006. Quantitative PCR to detect, discriminate and quantify intracellular parasites in their host: an example from three microsporidians in *Daphnia*. *Parasitology*, **133**:11–18.
- Refardt, D. & Ebert, D. 2007. Inference of parasite local adaptation using two different fitness components. *J. Evol. Biol.*, **20**:921–929.
- Refardt, D., Canning, E. U., Mathis, A., Cheney, S. A., Lafranchi-Tristem, N. J. & Ebert, D. 2002. Small subunit ribosomal DNA phylogeny of microsporidia that infect *Daphnia* (Crustacea: Cladocera). *Parasitology*, **124**:381–389.
- Ronquist, F. & Huelsenbeck, J. P. 2003. MrBayes 3: Bayesian phylogenetic inference under mixed models. *Bioinformatics*, **19**:1572–1574.
- Simakova, A. V., Pankova, T. F., Tokarev, Y. S. & Issi, I. V. 2005. *Senoma* gen. n., a new genus of microsporidia, with the type species *Senoma globulifera* comb. n. (syn. *Issia globulifera* Issi & Pankova 1983) from the malaria mosquito *Anopheles messeae* Fall. *Protistology*, **4**:135–144.

http://doc.rero.ch

- Sprague, V. 1977. Systematics of the Microsporidia. In: Bulla, L. A. & Cheng, T. C. (ed.), Comparative Pathobiology. Vol. 2: Systematics of the Microsporidia. Plenum Press, New York. p. 1–510.
- Sprague, V., Becnel, J. J. & Hazard, E. I. 1992. Taxonomy of phylum microspora. *Crit. Rev. Microbiol.*, **18**:285–395.
- Stirnadel, H. A. & Ebert, D. 1997. Prevalence, host specificity and impact on host fecundity of microparasites and epibionts in three sympatric *Daphnia* species. *J. Anim. Ecol.*, **66**:212–222.
- Swofford, D. L. 2003. PAUP*. Phylogenetic Analysis Using Parsimony (*and Other Methods). Version 4. Sinauer Associates, Sunderland, MA.
- Thompson, J. D., Higgins, D. G. & Gibson, T. J. 1994. CLUSTAL W: improving the sensitivity of progressive multiple sequence alignment through sequence weighting, position-specific gap penalties and weight matrix choice. *Nucleic Acids Res.*, **22**:4673–4680.
- Vávra, J. 1964. A failure to produce an artificial infection in cladoceran Microsporidia. *J. Protozool.*, **11**:S35–S36.
- Vávra, J. & Larsson, J. I. R. 1994. *Berwaldia schaefernai* (Jírovec, 1937) comb. n. (Protozoa, Microsporida), fine structure, life cycle and relationship to *Berwaldia singularis* Larsson, 1981. *Eur. J. Protistol.*, **30**:45–54.
- Vávra, J. & Larsson, J. I. R. 1999. Structure of the Microsporidia. In: Wittner, M. & Weiss, L. M. (ed.), The Microsporidia and Microsporidiosis. ASM Press, Washington, DC. p. 7–84.
- Vávra, J. & Maddox, J. V. 1976. Methods in microsporidiology. In: Bulla, L. A. & Cheng, T. C. (ed.), Comparative Pathobiology. Vol. 1: Biology of the Microsporidia. Plenum Press, New York. p. 281–319.
- Vávra, J., Hyliš, M., Oborník, M. & Vossbrinck, C. R. 2005. Microsporidia in aquatic microcrustacea: the copepod microsporidium *Marssoniella elegans* Lemmermann, 1900 revisited. *Folia Parasitol.* **52**:163–172.
- Vidtman, S. S. & Sokolova, Y. Y. 1994. The description of the new genus *Larssonia* gen. n. based on the ultrastructural analysis of *Microsporidium (Pleistophora) obtusa* from *Daphnia pulex*. *Parazitologiya*, **28**:202–213.
- Voronin, V. N. 1995. On the possible use of host-specific microsporidia (Protozoa) in the analysis of systematic relationships among Cladocera. *Zool. Zh.* **74**:17–21.
- Vossbrinck, C. R. & Debrunner-Vossbrinck, B. A. 2005. Molecular phylogeny of the Microsporidia: ecological, ultrastructural and taxonomic considerations. *Folia Parasitol.*, **52**:131–142.
- Vossbrinck, C. R., Andreadis, T. G., Vávra, J. & Becnel, J. J. 2004. Molecular phylogeny and evolution of mosquito parasitic microsporidia (Microsporidia: Amblyosporidae). *J. Eukaryot. Microbiol.*, **51**:88–95.
- Weiser, J. 1977. Contribution to the classification of Microsporidia. *Vestn. Cesk. Spol. Zool.* **41**:308–321.
- Williams, B. A. P., Cali, A., Takvorian, P. M. & Keeling, P. J. 2008. Distinct localization patterns of two putative mitochondrial proteins in the microsporidian *Encephalitozoon cuniculi*. *J. Eukaryot. Microbiol.* **55**:131–133.